ACSNANO
www.acsnano.org
ARTICLE

High Packing Density Unidirectional Arrays of Vertically Aligned Graphene with Enhanced Areal Capacitance for High-Power Micro-Supercapacitors

Shuanghao Zheng,[†,‡,⊥] Zhilin Li,[§,⊥] Zhong-Shuai Wu,*[,†] Yanfeng Dong,[†] Feng Zhou,[†] Sen Wang,[†,⊥] Qiang Fu,[†,‡] Chenglin Sun,[†] Liwei Guo,*[,§] and Xinhe Bao[†,‡]

[†]Dalian National Laboratory for Clean Energy and [‡]State Key Laboratory of Catalysis, Dalian Institute of Chemical Physics, Chinese Academy of Sciences, 457 Zhongshan Road, Dalian 116023, People's Republic of China

[§]Research & Development Center for Functional Crystals, Beijing National Laboratory for Condensed Matter Physics, Institute of Physics, Chinese Academy of Sciences, P.O. Box 603, Beijing 100190, People's Republic of China

[⊥]University of Chinese Academy of Sciences, 19 A Yuquan Road, Shijingshan District, Beijing 100049, People's Republic of China

Supporting Information

ABSTRACT: **Interfacial integration of a shape-engineered electrode with a strongly bonded current collector is the key for minimizing both ionic and electronic resistance and then developing high-power supercapacitors. Herein, we demonstrated the construction of high-power micro-supercapacitors (VG-MSCs) based on high-density unidirectional arrays of vertically aligned graphene (VG) nanosheets, derived from a thermally decomposed SiC substrate. The as-grown VG arrays showed a standing basal plane orientation grown on a $(000\bar{1})$ SiC substrate, tailored thickness (3.5−28 μm), high-density structurally ordering alignment of graphene consisting of 1−5 layers, vertically oriented edges, open intersheet channels, high electrical conductivity (192 S cm^{-1}), and strong bonding of the VG edges to the SiC substrate. As a result, the demonstrated VG-MSCs displayed a high areal capacitance of ∼7.3 mF cm^{-2} and a fast frequency response with a short time constant of 9 ms. Furthermore, VG-MSCs in both an aqueous polymer gel electrolyte and nonaqueous ionic liquid of 1-ethyl-3-methylimidazolium tetrafluoroborate operated well at high scan rates of up to 200 V s^{-1}. More importantly, VG-MSCs offered a high power density of ∼15 W cm^{-3} in gel electrolyte and ∼61 W cm^{-3} in ionic liquid. Therefore, this strategy of producing high-density unidirectional VG nanosheets directly bonded on a SiC current collector demonstrated the feasibility of manufacturing high-power compact supercapacitors.**

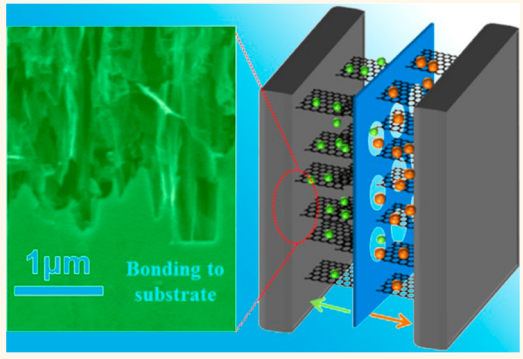

KEYWORDS: *vertically aligned, graphene, high power, micro-supercapacitors, on-chip, energy storage, electrochemical capacitors*

The ever-increasing demand of multifunctional integrated circuitry has spawned an enthusiastic quest for efficient, miniaturized, compact energy storage devices.[1,2] The micro-supercapacitors (MSCs) with appealing characteristics of high power density, fast charge and discharge rate, and long lifetime are gradually acknowledged as a discrete microscale power source for directly integrating microelectronic systems on-chip.[3−5] Until now, tremendous efforts have been devoted to improving the power and energy densities of MSCs through developing nanostructured electrode materials. Specifically, the pseudocapacitive metal oxides/hydroxides (*e.g.*, RuO_2,[6,7] MnO_2,[8,9] Co_3O_4,[10] $Ni(OH)_2$[11]), polymers (*e.g.*, polyaniline,[12] polypyrrole,[13] polythiophene[14]), silicon nanowires,[15] and MXene[16,17] are mainly targeted for high volumetric capacitance MSCs, while electric double-layer capacitive nanocarbons, such as activated carbon (AC),[18,19] carbide-derived carbon (CDC),[3,20] onion-like carbon (OLC),[21] and carbon nanotubes (CNTs),[22,23] are intensively exploited for high-power MSCs with long cyclability and fast frequency response. However, the complex porous structure of most nanocarbon electrodes and strong restacking of graphene nanosheets negatively impacts high-power handling characteristics of MSCs because of the long path of ion diffusion.[24]

Received: January 24, 2017
Accepted: March 23, 2017
Published: March 23, 2017

DOI: 10.1021/acsnano.7b00553
ACS Nano 2017, 11, 4009−4016

Scheme 1. Schematic illustration of the fabricated VG-MSCs using VG films derived from the SiC substrates.

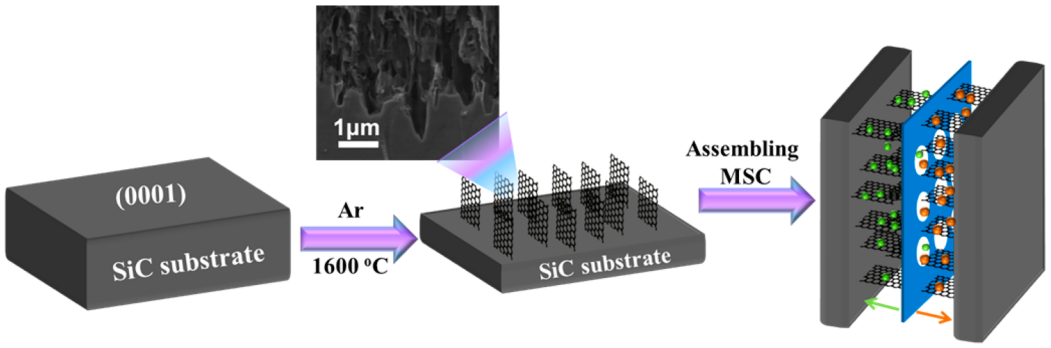

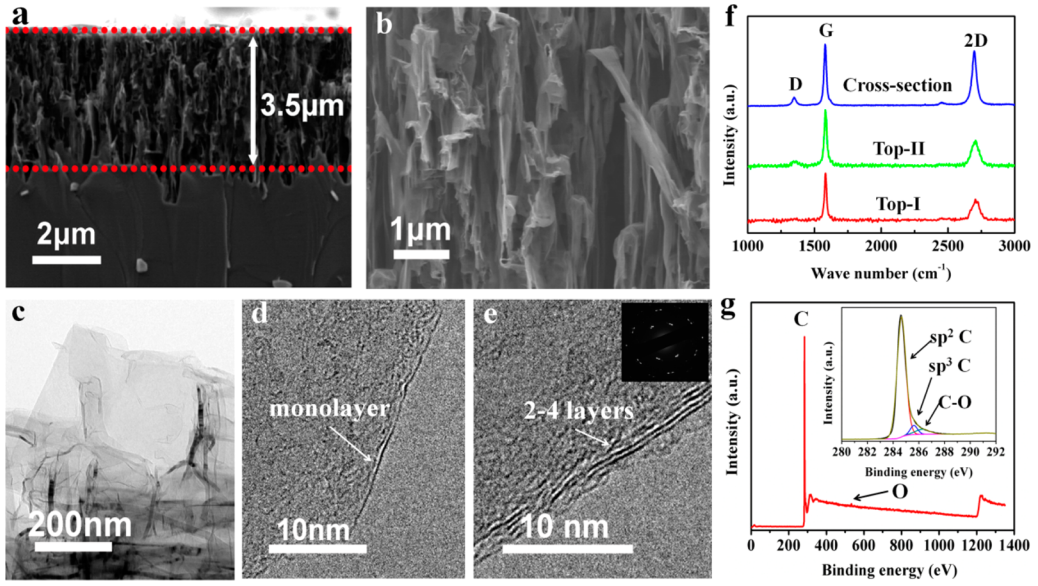

Figure 1. Morphology and structure of VG. (a, b) Cross-section SEM images in low magnification (a) and high magnification (b). (c) TEM image and (d, e) HRTEM images of (d) monolayer and (e) multilayer VG. Inset in (e) is a SAED image. (f) Raman spectra from top and cross-section views. (g) XPS full spectrum. Inset is the deconvoluted C 1s XPS spectrum.

To realize high-power MSCs, designing a shape-engineered electrode with short channel lengths and easy accessibility of electrolyte ions as well as strong interfacial interaction between electrode and current collector is an important and necessary requirement.[22] In light of this, the power performance of oriented nanostructured materials with a uniform spatial alignment for thin-film MSCs can significantly outperform their nonoriented counterparts.[25] Special emphasis is given to vertically aligned or oriented graphene (VG) nanosheets with features of high electrical conductivity, open intersheet channels, and edge-enriched structure for high-power MSCs in a stacked cell, which is superior to horizontally, randomly stacked graphenes.[26] For instance, VG films manufactured by a hand-rolling and cutting process displayed a remarkable volumetric capacitance of 123 F cm^{-3} at a high current density of 20 A g^{-1}, while randomly dispersed graphene powder and horizontally stacked film had a negligible capacitance at such rate.[26] Very impressively, supercapacitors made from VG nanosheets grown directly on metal current collectors (Ni) disclosed an ac line-filtering performance having an RC time constant of only 200 μs.[27,28] This was attributed to the advanced design of strong interaction between VG edges and its supporting conductive substrate, which significantly minimized both ionic and electronic resistance, ideally suited for producing high-power supercapacitors. Unfortunately, these VG nanosheets that are usually grown by radio frequency plasma-enhanced chemical vapor deposition (PECVD) show entangled and disordered networks with a low packing density, typically an interlayer distance of a few hundred nanometers.[29−32] Moreover, high cost and complicated manufacturing procedures of PECVD systems could eventually hinder large-scale production of VG for actual use.[25,33] As an appealing method, thermal decomposition of a SiC substrate in high vacuum developed by Gogotsi's group pioneered the growth of high packing density VG nanosheets standing normally to the surface.[34] However, the designed fabrication of high-density unidirectional VG directly grown on a SiC substrate for high-power supercapacitors has not been fully exploited.

Herein, we reported the construction of high-power MSCs (denoted as VG-MSCs) based on high-density unidirectional arrays of VG nanosheets derived from a thermally decomposed SiC substrate, operating in both an aqueous gel and nonaqueous ionic liquid electrolytes (Scheme 1). The VG arrays with a standing basal plane orientation and tailored thickness were grown on a $(000\bar{1})$ SiC substrate at 1600 °C for 0.5 or 2 h in a vacuum ambient with physical vapor transport (PVT) equipment and showed a high-density structurally ordering alignment of monolayer and few-layer (2−5 layers)

DOI: 10.1021/acsnano.7b00553
ACS Nano 2017, 11, 4009−4016

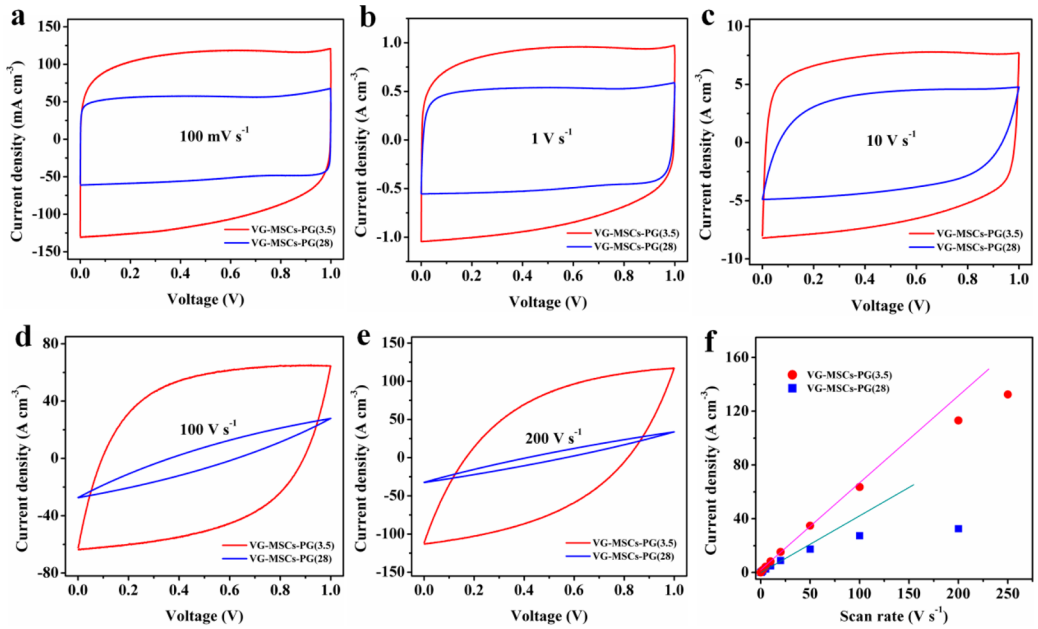

Figure 2. CV curves of VG-MSCs-PG(3.5) and VG-MSCs-PG(28). (a–e) CV curves obtained at various scan rates of (a) 0.1, (b) 1, (c) 10, (d) 100, and (e) 200 V s^{-1}. (h) Discharge current density as a function of scan rate.

graphene nanosheets. Because of the vertically oriented enriched edges, open intersheet channels, high electrical conductivity (192 S cm^{-1}), and strong bonding of the VG edges to the SiC substrate, the fabricated VG-MSCs displayed a high areal capacitance of ~7.3 mF cm^{-2}, a volumetric capacitance of ~4.6 F cm^{-3}, and a fast frequency response with a short time constant of 9 ms. Remarkably, VG-MSCs working in both a polymer gel electrolyte of H_2SO_4/poly(vinyl alcohol) (H_2SO_4/PVA) and an ionic liquid of 1-ethyl-3-methylimidazolium tetrafluoroborate ($EMIMBF_4$) worked well at a high scan rate of up to 200 V s^{-1}. More significantly, VG-MSCs showed a high power density of ~15 W cm^{-3} in gel electrolyte and ~61 W cm^{-3} in ionic liquid as well as remarkable long-term cycling stability.

RESULTS AND DISCUSSION

The morphology of the as-grown VG nanosheets derived from thermal decomposition of the SiC substrate (see details in the Experimental Section) was examined by scanning electron microscopy (SEM) and transmission electron microscopy (TEM) measurements (Figure 1 and Figure S1). Cross-section SEM images of VG films showed uniform and tailored thickness of ~3.5 and ~28 μm by changing the etching time, and importantly the array of VG nanosheets preferred a perpendicular alignment to the surface of the thermally decomposed SiC substrate (Figure 1a, Figure S1a). A high-magnification SEM image (Figure 1b) presented a high packing density of VG nanosheets that were physically overlapped or partly bonding along the growth direction of the SiC ($000\bar{1}$) plane. It is noteworthy that, from the magnified observation of the interface region, a strong bonding interaction was observed between the fresh growth end of graphene edges and the frontal surface of the SiC substrate, which is the key for minimizing the interfacial electronic resistance and achieving high-power supercapacitors (Figure S1b). Furthermore, top-view SEM images exhibited the appearance of numerous irregular hollows (Figure S1c,d) and further revealed the alignment of graphene basal planes with a uniform height. This is ascribed to the tremendous difference in saturation pressure between silicon and carbon atoms, about 10^6 at 1600 °C. In this case, the silicon atoms near the surface of the SiC substrate are rapidly evaporated out, and the remaining carbon atoms are constructed into structurally aligned graphene nanosheets on the SiC substrate.[34−36] As the process proceeded, the height of the VG arrays gradually increased. TEM images (Figure 1c) showed the nature of atomically thin, flat, transparent nanosheets, consisting of monolayer and few-layer graphene (2–5 layers), as identified from the exposed edges by high-resolution TEM (HRTEM, Figure 1d,e).

The structural quality of the VG arrays was further investigated by Raman spectroscopy and X-ray photoelectron spectroscopy (XPS). As shown in Figure 1f and Figure S1d, Raman spectra exhibited two characteristic peaks of G and 2D bands located at 1584 and 2706 cm^{-1}, respectively. Notably, a very weak D peak at 1353 cm^{-1}, corresponding to a low I_D/I_G ratio of 0.15, was observable from the cross-section of the VG film, but no D peak (top-I) and a lower I_D/I_G ratio of 0.08 (top-II) were detected from the top plane of the film, demonstrative of high quality of the as-grown VG nanosheets. This was also confirmed by XPS results (Figure 1g), which exhibited a distinguishable C signal at 284.6 eV, corresponding to a major carbon content of as high as ~96.4%, and a negligible weak peak of oxygen at 532 eV, only ~3.6%, mainly resulting from the absorption of oxygen in air. Additionally, the as-grown VG films, measured by a standard four-point probe system, displayed exceptional electrical conductivity, *e.g.*, ~192 S cm^{-1} for 3.5-μm-thick VG film and 87 S cm^{-1} for 28-μm-thick VG film, highlighting the efficient production of high-conductive VG films by thermal decomposition of SiC substrates.

To highlight high-power performance, we first assembled all-solid-state VG-MSCs sandwiched H_2SO_4/PVA polymer gel electrolyte between two pieces of 3.5-μm-thick VG film on a SiC substrate (denoted as VG-MSCs-PG(3.5)). To investigate the effect of film thickness, we also constructed VG-MSCs based on 28-μm-thick VG films with the same procedure

DOI: 10.1021/acsnano.7b00553
ACS Nano 2017, 11, 4009–4016

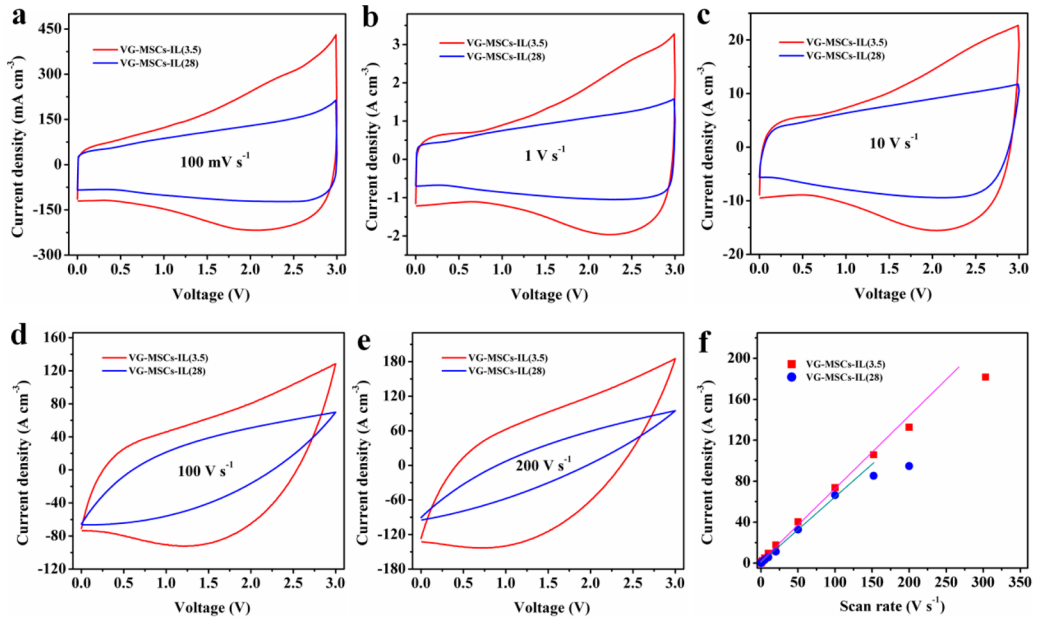

Figure 3. CV curves of VG-MSCs-IL(3.5) and VG-MSCs-IL(28). (a–e) CV curves obtained at various scan rates of (a) 0.1, (b) 1, (c) 10, (d) 100, and (e) 200 V s^{-1}. (f) Discharge current density as a function of scan rate.

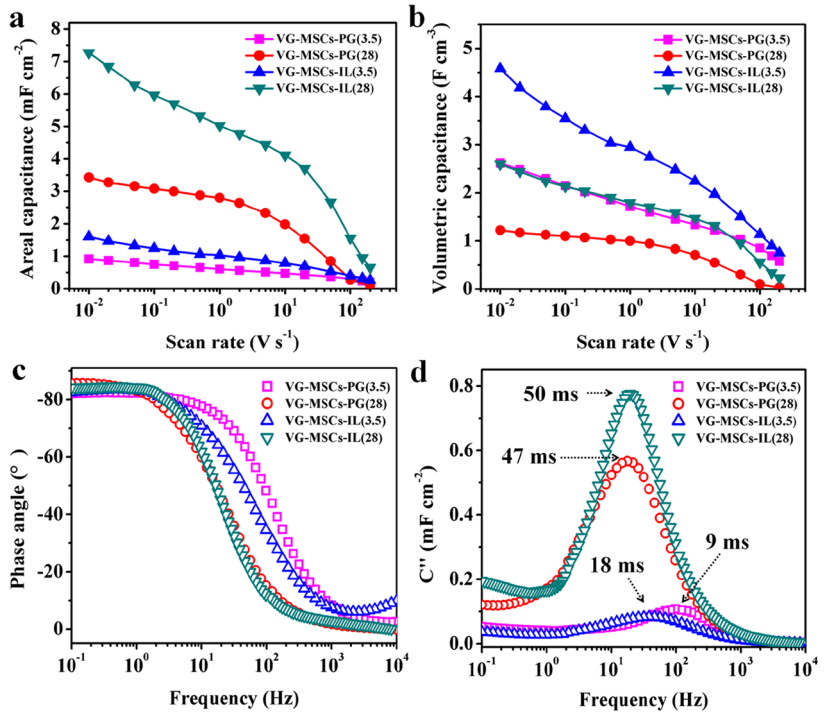

Figure 4. Performance comparison of VG-MSCs-PG(3.5), VG-MSCs-PG(28), VG-MSCs-IL(3.5), and VG-MSCs-IL(28). (a) Areal capacitance, (b) volumetric capacitance, (c) Bode plots, and (d) evolution of the imaginary capacitance.

(denoted as VG-MSCs-PG(28)). Then, cyclic voltammetry (CV) was carried out at various scan rates from 1 mV s^{-1} to 200 V s^{-1} (Figure 2a–e, Figure S2a,b). Clearly, it was observed that both VG-MSCs-PG(3.5) and VG-MSCs-PG(28) exhibited a typical electric double-layer capacitive feature with a nearly rectangular CV shape in lower scan rates from 1 to 1000 mV s^{-1} (Figure 2a,b; Figure S2a,b). With increasing scan rate, VG-MSCs-PG(3.5) still maintained higher volumetric current densities and better capacitive CV shapes in comparison with VG-MSCs-PG(28) (Figure 2c–e). This disparity could be explained by higher electric conductivity and shorter ionic paths of the thinner VG film. Note that a linear dependence of the discharge current as a function of scan rate was recognized at 100 V s^{-1} for VG-MSCs-PG(3.5) (Figure 2f), suggestive of high instantaneous power. Remarkably, VG-MSCs-PG(3.5) allowed for operation at a high scan rate of up to 200 V s^{-1} (Figure 2e), which is at least one order of magnitude higher than those supercapacitors based on horizontally stacked graphene film (10 V s^{-1})[37] and randomly dispersed graphene

DOI: 10.1021/acsnano.7b00553
ACS Nano 2017, 11, 4009–4016

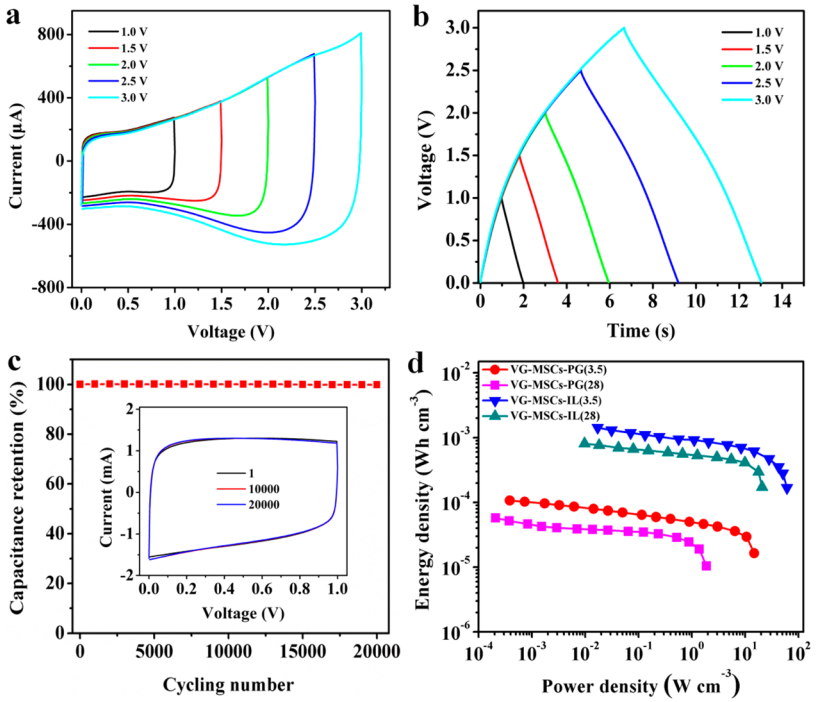

Figure 5. Electrochemical characterization of VG-MSCs. (a) CV curves of VG-MSCs-IL(3.5) at different voltages from 1 to 3 V. (b) GCD curves of VG-MSCs-IL(3.5) at different voltages from 1 to 3 V. (c) Cycling stability of VG-MSCs-PG(3.5). Inset is the first, 10 000th, and 20 000th CV curves. (d) Ragone plot of volumetric power density and energy density.

powder (1 V s^{-1})[38] and well comparable to other reported VG films for MSCs (Table S1).

Ionic liquids (ILs) with a large potential window up to 4 V are intensively applied as high-voltage electrolytes to boost the energy density of supercapacitors. However, due to the large molecular size, low ionic conductivity, and high viscosity, ionic-liquid-based supercapacitors generally manifest low power performance. In view of this, we also examined the electrochemical performance of as-fabricated VG-MSCs over a stable potential window of 3 V in an ionic liquid of $EMIMBF_4$ electrolyte (Figure 3, Figure S3). The corresponding VG-MSCs based on 3.5- and 28-μm-thick VG films were denoted as VG-MSCs-IL(3.5) and VG-MSCs-IL(28), respectively. Notably, CVs of both VG-MSCs-IL(3.5) and VG-MSCs-IL(28) displayed unpronounced double-layer capacitive behavior with quasi-rectangular shape at low scan rates (Figure 3a–c). Furthermore, it was demonstrated that VG-MSCs-IL(3.5) worked well at a high scan rate of up to 200 V s^{-1}, while VG-MSCs-IL(28) did not function at such rates (Figure 3d–f). This phenomenon is similar to the VG-MSCs-PG(3.5) and VG-MSCs-PG(28) in gel electrolyte.

The areal capacitance and volumetric capacitance of VG-MSCs-PG(3.5), VG-MSCs-PG(28), VG-MSCs-IL(3.5), and VG-MSCs-IL(28) are shown in Figure 4a and b. From Figure 4a, it was observed that VG-MSCs-PG(28) represented an areal capacitance of 3.4 mF cm^{-2} at 10 mV s^{-1}, which is much higher than that of VG-MSCs-PG(3.5) (0.9 mF cm^{-2}). This enhancement of areal capacitance is explained by the significant (28 μm) thickness of the VG film. Furthermore, it was found that ionic liquid-based VG-MSCs significantly boosted higher areal capacitance than those of polymer gel-based microdevices. Typically, VG-MSCs-IL(28) delivered an areal capacitance of 7.3 mF cm^{-2} at 10 mV s^{-1}, twice higher than that of VG-MSCs-PG(28). Remarkably, this value (7.3 mF cm^{-2}) was much higher than those of CVD-grown VG nanosheets (2 mF cm^{-2}),[39] reduced graphene oxide (0.5–2.5 mF cm^{-2}),[40] CDC (1.5 mF cm^{-2}),[41] OLC (1.7 mF cm^{-2}),[21] CNTs (0.5–1.5 mF cm^{-2}),[42] and other nanostructured electrodes of silicon nanowires (20–50 μF cm^{-2}),[43] silicon nanotrees (84 μF cm^{-2}),[44] and MXene (3.2 mF cm^{-2})[45] for MSCs.

As mentioned previously, areal capacitance and volumetric capacitance vary inversely with increasing film thickness regardless of the used electrolytes. In our case, we also observed that, upon increasing the film thickness, the volumetric capacitance at 10 mV s^{-1} decreased from 2.6 F cm^{-3} for VG-MSCs-PG(3.5) to 1.1 F cm^{-3} for VG-MSCs-PG(28) (Figure 4b). Similarly, 4.6 F cm^{-3} for VG-MSCs-IL(3.5) was reduced to 2.5 F cm^{-3} for VG-MSCs-IL(28) in ionic liquid. It should be emphasized that both VG-MSCs-PG(3.5) and VG-MSCs-IL(3.5) still kept a significant capacitance of 0.8 and 1.1 F cm^{-3}, respectively, at a high scan rate of 100 V s^{-1}. This result is attributed to the advanced architecture of unidirectional VG arrays seamlessly bonding to the conductive SiC substrate.

Electrochemical impedance spectra (EIS) confirmed fast ion transport of VG-MSCs in both polymer gel and ionic liquid electrolytes. For instance, VG-MSCs-PG(28) and VG-MSCs-IL(28) even with a 28-μm-thick VG film still exhibited a straight line with nearly closed −90° at low frequency and a quite small equivalent series resistance (ESR) in the high-frequency region (Figure 4c,d; Figure S4). Figure 4c reveals the dependence of phase angle on the frequency of VG-MSCs-PG(3.5), VG-MSCs-PG(28), VG-MSCs-IL(3.5), and VG-MSCs-IL(28). As can be seen, VG-MSCs-PG(3.5) at a phase angle of −45° showed a characteristic frequency (f_0) of 110 Hz, which is higher than that of VG-MSCs-IL(3.5) (56 Hz). Further, both of them are higher than those of VG-MSCs-PG(28) (21 Hz) and VG-MSCs-IL(28) (20 Hz). This is well

DOI: 10.1021/acsnano.7b00553
ACS Nano 2017, 11, 4009–4016

explained by (i) the better ionic conductivity in aqueous gel in comparison with ionic liquid and (ii) the higher electrical conductivity in the thin VG film (3.5 μm). Correspondingly, the relaxation time constant (τ_0) evaluated by the equation $\tau_0 = 1/f_0$ (the minimum time needed to discharge all the energy from the device at an efficiency of more than 50%) was ~9 ms for VG-MSCs-PG(3.5), ~18 ms for VG-MSCs-IL(3.5), ~47 ms for VG-MSCs-PG(28), and ~50 ms for VG-MSCs-IL(28). These values are much lower than those of the supercapacitors using AC (700 ms),[21] VG (290 ms),[39] vertical graphene forest (~250 ms),[46] and liquid-mediated graphene (200−73 ms),[47] and well comparable to the reported high-power supercapacitors based on vertically aligned CNTs (~21 ms)[48] and planar MSCs based on OLC (~26 ms)[21] (Table S1).

To investigate the effect of the voltage on the capacitance in ionic liquid, we further investigated the different voltages of VG-MSCs-IL(3.5) from 1 to 3 V by CVs at a scan rate of 1 V s^{-1} and galvanostatic charge−discharge (GCD) at a current density of 700 mA cm^{-3} (Figure 5a,b). Importantly, it was found that the integration area of CV curves and charge−discharge time of GCD profiles monotonically increased with increasing operating voltage window, indicative of capacitance enhancement (Figure S5). For instance, VG-MSCs-IL(3.5) at 1 V s^{-1} exhibited an increasing areal capacitance of 0.50 mF cm^{-2} at 1 V, 0.58 mF cm^{-2} at 1.5 V, 0.71 mF cm^{-2} at 2.0 V, 0.86 mF cm^{-2} at 2.5 V, and 1.0 mF cm^{-2} at 3.0 V (Figure S5a). This phenomenon of capacitance enhancement and nonlinear discharges of GCD profiles was mainly ascribed to the increasing effective accessible area of high packing density unidirectional VG arrays, consisting of tightly stacked graphene nanosheets (Figure 1a,b), by accommodating more electrolyte ions of the ionic liquid in high-voltage operation. On one hand, the ions can efficiently intercalate/diffuse into the narrower and deeper interlayer channels of adjacent tightly stacked graphene nanosheets under high voltage (Figure 5b). On the other hand, the open intersheet channels, like "flexible pores", can sufficiently accommodate the increased ions for charge storage at high voltage. In addition, VG-MSCs-PG(3.5) in gel electrolyte showed excellent cycling stability without any capacitance degradation after 20 000 times at a scan rate of 5 V s^{-1} (Figure 5c). VG-MSCs-IL(3.5) retained 83% of its initial capacitance after 10 000 times in ionic liquid (Figure S6a), which was mainly attributed to the increased internal resistance upon cycling (Figure S6b−i). Although the cyclability of VG-MSCs-IL(3.5) is lower than that of VG-MSCs-PG(3.5), it is also very impressive taking into account the higher working voltage and capacitance achieved in VG-MSCs-IL(3.5).

The Ragone plot in Figure 5d compares the volumetric performance of VG-MSCs-PG(3.5), VG-MSCs-PG(28), VG-MSCs-IL(3.5), and VG-MSCs-IL(28). Our VG-MSCs-IL(3.5) delivered a volumetric energy density of ~1.4 mWh cm^{-3}, higher than that of VG-MSCs-IL(28) (0.8 mWh cm^{-3}) and one order of magnitude higher than those of VG-MSCs-PG(3.5) (0.1 mWh cm^{-3}) and VG-MSCs-PG(28) (0.06 mWh cm^{-3}). Remarkably, it should be noted that VG-MSCs-(3.5) offered a high volumetric power density of ~15 W cm^{-3} in gel electrolyte and ~61 W cm^{-3} in ionic liquid.

The excellent performance of VG-MSCs-IL(3.5) is attributed to the extraordinary unidirectional structure of VG arrays derived from the SiC substrate with seamless integration with each other. Unlike the conventional stacked electrode used in supercapacitors, wherein the graphene layers have random or horizontal orientation with respect to the current collectors, in our design graphene edges are vertically aligned on the conductive current collector (SiC substrate) for fast ion diffusion, short diffusion paths, and large electroactive accessible area. Very importantly, seamless integration of VG arrays strongly bonding with the current collectors (SiC substrate) is the key for minimizing the contact resistance, endowing rapid ion and electron transport for ultrafast charge and discharge. In sharp contrast, the interaction of active materials (*e.g.*, graphene) with current collectors in the conventional electrode is a relatively weak contact, usually implemented by extra physical pressure force, resulting in poor rate capability. Moreover, the high packing density of vertically oriented exposed edges is another critical factor to boost the great enhancement of the capacitance and energy density.

CONCLUSIONS

In summary, we have demonstrated the fabrication of high-power MSCs based on high-density unidirectional VG arrays directly derived from a thermally decomposed SiC substrate. The resulting VG arrays presented high-density structurally ordered alignment of monolayer and few-layer graphene nanosheets, edge-enriched structure, open intersheet channels, high electrical conductivity, and strong bonding of the VG edges to the SiC substrate. The fabricated VG-MSCs displayed high areal capacitance and volumetric capacitance, fast frequency response, and excellent long-term cyclability. Remarkably, VG-MSCs in both gel electrolyte and ionic liquid can operate well at a high scan rate of up to 200 V s^{-1} and showed a high power density of ~61 W cm^{-3}. Therefore, we believed that this technique of thermal decomposition of a SiC substrate is promising for large-scale production of high-density VG arrays with strong bonding to the conductive substrate and subsequently for their direct integration into high-power supercapacitors with miniaturized electronics.

EXPERIMENTAL SECTION

Synthesis of VG. The VG nanosheets were grown on a SiC substrate with a PVT system, as reported in our previous work.[35] Highly nitrogen-doped on-axis C-face 6H-SiC substrates with a size of 2 × 1 cm (Tanke-Blue, Beijing) were applied for the VG growth. First, SiC substrates were placed in a high-purity graphite crucible with the C-face at the top side, and the crucible was loaded into the growth chamber. Induction-coupling heating was adopted to raise the growth temperature to about 1600 °C in 3 h under an argon ambient with a pressure of about 30 kPa. After that the growth chamber was pumped to a vacuum ambient in a pressure of less than 10^{-3} Pa, and the conditions were kept for about 0.5 or 2 h for different VG samples. Finally, the growth system was refilled with argon gas to a pressure of about 30 kPa and naturally cooled to room temperature. VG arrays with a tailored height grown on the SiC substrates were obtained.

Characterization. The morphologies of VGs were determined by field emission SEM (FE-SEM, JSM-7800F) with an accelerating voltage of 3 kV and TEM (JEM-2100) operated at 200 kV. The Raman spectrum was obtained from a LabRAM HR 800 Raman spectrometer with 532 nm laser excitation in an air atmosphere. XPS measurement was conducted on a Thermo ESCALAB 250Xi (monochromated Al Kα, 1486.6 eV, 15 kV) with a high vacuum of 10^{-7} Pa. The electric conductivity was measured by a standard four-point probe system (RTS-9).

Assembly and Electrochemical Measurement. For all-solid-state VG-MSCs (VG-MSCs-PG(3.5), VG-MSCs-PG(28)) using H_2SO_4/PVA as gel electrolyte and separator, the VG films were immersed into the gel electrolyte and kept for 30 s. After the H_2SO_4/PVA gel electrolyte solidified, two electrolyte-coated VG film electrodes were carefully symmetrically assembled together. Finally,

DOI: 10.1021/acsnano.7b00553
ACS Nano 2017, 11, 4009−4016

the all-solid-state VG-MSCs were obtained. For ionic-liquid-based VG-MSCs (VG-MSCs-IL(3.5), VG-MSCs-IL(28)) using $EMIMBF_4$ as electrolyte, VG-MSCs were assembled by sandwiching an electrolyte-immerged ion-porous separator (Celgard 3501) between two pieces of VG films in an argon-filled glovebox with H_2O and O_2 less than 0.5 ppm. The electrochemical performance of the as-fabricated VG-MSCs was obtained in an electrochemical workstation (CHI 760E) using CV, GCD, and EIS measurements at room temperature. CV curves were tested at various scan rates from 0.001 to 300 V s^{-1}. GCD profiles were measured at varying current densities from 0.005 to 40 A cm^{-3}. EIS spectra were recorded in the frequency range from 0.1 Hz to 100 kHz with a 5 mV ac amplitude.

ASSOCIATED CONTENT

Supporting Information

The Supporting Information is available free of charge on the ACS Publications website at DOI: 10.1021/acsnano.7b00553.

Additional detailed calculations, tables, figures of the morphology of VG, CV curves, Nyquist plots, areal capacitance, and cycling stability (PDF)

AUTHOR INFORMATION

Corresponding Authors

*E-mail: wuzs@dicp.ac.cn (Z.-S.Wu).
*E-mail: lwguo@iphy.ac.cn (L.W. Guo).

ORCID

Zhong-Shuai Wu: 0000-0003-1851-4803
Qiang Fu: 0000-0001-5316-6758
Xinhe Bao: 0000-0001-9404-6429

Author Contributions

Z.S.W., L.W.G., and X.H.B. proposed and supervised the overall project. S.H.Z. did the fabrication and electrochemical measurement of MSCs. S.H.Z. and Z.S.W. analyzed the data. Z.L.L., Q.F., and L.W.G prepared the VG. Y.F.D., F.Z., S.W., and C.L.S participated in the preparation of electrolytes and the characterization of the related materials. S.H.Z., Z.S.W., L.W.G., Q.F., C.L.S., and X.H.B wrote the paper. All authors discussed the results and commented on the manuscript. All authors have given approval to the final version of the manuscript.

Notes

The authors declare no competing financial interest.

ACKNOWLEDGMENTS

This work was financially supported by the National Natural Science Foundation of China (Grant 51572259), Ministry of Science and Technology of China (Grants 2016YBF0100100 and 2016YFA0200200), Natural Science Foundation of Liaoning Province (Grant 201602737), Thousand Youth Talents Plan of China, DICP (Grant Y5610121T3), China Postdoctoral Science Foundation (Grant 2016M601349), and dedicated funds for methanol conversion from DICP.

REFERENCES

(1) Simon, P.; Gogotsi, Y. Materials for Electrochemical Capacitors. *Nat. Mater.* **2008**, *7*, 845−854.
(2) Rogers, J. A.; Someya, T.; Huang, Y. Materials and Mechanics for Stretchable Electronics. *Science* **2010**, *327*, 1603−1607.
(3) Chmiola, J.; Largeot, C.; Taberna, P. L.; Simon, P.; Gogotsi, Y. Monolithic Carbide-Derived Carbon Films for Micro-Supercapacitors. *Science* **2010**, *328*, 480−483.
(4) Kyerematen, N. A.; Brousse, T.; Pech, D. Microsupercapacitors as Miniaturized Energy-Storage Components for On-Chip Electronics. *Nat. Nanotechnol.* **2017**, *12*, 7−15.
(5) Qi, D.; Liu, Y.; Liu, Z.; Zhang, L.; Chen, X. Design of Architectures and Materials in In-Plane Micro-Supercapacitors: Current Status and Future Challenges. *Adv. Mater.* **2017**, *29*, 1602802.
(6) Wu, Z. S.; Wang, D. W.; Ren, W.; Zhao, J.; Zhou, G.; Li, F.; Cheng, H. M. Anchoring Hydrous RuO_2 on Graphene Sheets for High-Performance Electrochemical Capacitors. *Adv. Funct. Mater.* **2010**, *20*, 3595−3602.
(7) Xu, J.; Wang, Q. F.; Wang, X. W.; Xiang, Q. Y.; Hang, B.; Chen, D.; Shen, G. Z. Flexible Asymmetric Supercapacitors Based upon Co_9S_8 Nanorod//Co_3O_4@RuO_2 Nanosheet Arrays on Carbon Cloth. *ACS Nano* **2013**, *7*, 5453−5462.
(8) Lu, X. H.; Zheng, D. Z.; Zhai, T.; Liu, Z. Q.; Huang, Y. Y.; Xie, S. L.; Tong, Y. X. Facile Synthesis of Large-Area Manganese Oxide Nanorod Arrays as a High-Performance Electrochemical Supercapacitor. *Energy Environ. Sci.* **2011**, *4*, 2915−2921.
(9) Xu, P.; Wei, B. Q.; Cao, Z. Y.; Zheng, J.; Gong, K.; Li, F. X.; Yu, J. Y.; Li, Q. W.; Lu, W. B.; Byun, J. H.; et al. Stretchable Wire-Shaped Asymmetric Supercapacitors Based on Pristine and MnO_2 Coated Carbon Nanotube Fibers. *ACS Nano* **2015**, *9*, 6088−6096.
(10) Dong, X. C.; Xu, H.; Wang, X. W.; Huang, Y. X.; Chan-Park, M. B.; Zhang, H.; Wang, L. H.; Huang, W.; Chen, P. 3D Graphene-Cobalt Oxide Electrode for High-Performance Supercapacitor and Enzymeless Glucose Detection. *ACS Nano* **2012**, *6*, 3206−3213.
(11) Wang, H. L.; Casalongue, H. S.; Liang, Y. Y.; Dai, H. J. $Ni(OH)_2$ Nanoplates Grown on Graphene as Advanced Electrochemical Pseudocapacitor Materials. *J. Am. Chem. Soc.* **2010**, *132*, 7472−7477.
(12) Wu, Z. S.; Parvez, K.; Li, S.; Yang, S.; Liu, Z. Y.; Liu, S. H.; Feng, X. L.; Muellen, K. Alternating Stacked Graphene-Conducting Polymer Compact Films with Ultrahigh Areal and Volumetric Capacitances for High-Energy Micro-Supercapacitors. *Adv. Mater.* **2015**, *27*, 4054−4061.
(13) Zhu, M.; Huang, Y.; Deng, Q.; Zhou, J.; Pei, Z.; Xue, Q.; Huang, Y.; Wang, Z.; Li, H.; Huang, Q.; Zhi, C. Highly Flexible, Freestanding Supercapacitor Electrode with Enhanced Performance Obtained by Hybridizing Polypyrrole Chains with MXene. *Adv. Energy Mater.* **2016**, *6*, 1600969.
(14) Zhai, D. Y.; Li, B. H.; Du, H. D.; Gao, G. Y.; Gan, L.; He, Y. B.; Yang, Q. H.; Kang, F. Y. The Preparation of Graphene Decorated with Manganese Dioxide Nanoparticles by Electrostatic Adsorption for Use in Supercapacitors. *Carbon* **2012**, *50*, 5034−5043.
(15) Peng, K. Q.; Wang, X.; Li, L.; Hu, Y.; Lee, S. T. Silicon Nanowires for Advanced Energy Conversion and Storage. *Nano Today* **2013**, *8*, 75−97.
(16) Ghidiu, M.; Lukatskaya, M. R.; Zhao, M.-Q.; Gogotsi, Y.; Barsoum, M. W. Conductive Two-Dimensional Titanium Carbide 'Clay' with High Volumetric Capacitance. *Nature* **2014**, *516*, 78−81.
(17) Zhao, M.-Q.; Ren, C. E.; Ling, Z.; Lukatskaya, M. R.; Zhang, C.; Van Aken, K. L.; Barsoum, M. W.; Gogotsi, Y. Flexible MXene/Carbon Nanotube Composite Paper with High Volumetric Capacitance. *Adv. Mater.* **2015**, *27*, 339−345.
(18) Kim, H.; Cho, M. Y.; Kim, M. H.; Park, K. Y.; Gwon, H.; Lee, Y.; Roh, K. C.; Kang, K. A Novel High-Energy Hybrid Supercapacitor with an Anatase TiO_2-Reduced Graphene Oxide Anode and an Activated Carbon Cathode. *Adv. Energy Mater.* **2013**, *3*, 1500−1506.
(19) Lam, D. V.; Jo, K.; Kim, C.-H.; Kim, J.-H.; Lee, H.-J.; Lee, S.-M. Activated Carbon Textile *via* Chemistry of Metal Extraction for Supercapacitors. *ACS Nano* **2016**, *10*, 11351−11359.
(20) Huang, P.; Lethien, C.; Pinaud, S.; Brousse, K.; Laloo, R.; Turq, V.; Respaud, M.; Demortière, A.; Daffos, B.; Taberna, P. L.; et al. On-Chip and Freestanding Elastic Carbon Films for Micro-Supercapacitors. *Science* **2016**, *351*, 691−695.
(21) Pech, D.; Brunet, M.; Durou, H.; Huang, P. H.; Mochalin, V.; Gogotsi, Y.; Taberna, P. L.; Simon, P. Ultrahigh-Power Micrometre-Sized Supercapacitors Based on Onion-Like Carbon. *Nat. Nanotechnol.* **2010**, *5*, 651−654.
(22) Futaba, D. N.; Hata, K.; Yamada, T.; Hiraoka, T.; Hayamizu, Y.; Kakudate, Y.; Tanaike, O.; Hatori, H.; Yumura, M.; Iijima, S. Shape-Engineerable and Highly Densely Packed Single-Walled Carbon

DOI: 10.1021/acsnano.7b00553
ACS Nano 2017, 11, 4009−4016

Nanotubes and Their Application as Super-Capacitor Electrodes. *Nat. Mater.* **2006**, *5*, 987−994.
(23) Kaempgen, M.; Chan, C. K.; Ma, J.; Cui, Y.; Gruner, G. Printable Thin Film Supercapacitors Using Single-Walled Carbon Nanotubes. *Nano Lett.* **2009**, *9*, 1872−1876.
(24) Yoo, J. J.; Balakrishnan, K.; Huang, J.; Meunier, V.; Sumpter, B. G.; Srivastava, A.; Conway, M.; Mohana Reddy, A. L.; Yu, J.; Vajtai, R.; Ajayan, P. M. Ultrathin Planar Graphene Supercapacitors. *Nano Lett.* **2011**, *11*, 1423−1427.
(25) Bo, Z.; Mao, S.; Han, Z. J.; Cen, K. F.; Chen, J. H.; Ostrikov, K. Emerging Energy and Environmental Applications of Vertically-Oriented Graphenes. *Chem. Soc. Rev.* **2015**, *44*, 2108−2121.
(26) Yoon, Y.; Lee, K.; Kwon, S.; Seo, S.; Yoo, H.; Kim, S.; Shin, Y.; Park, Y.; Kim, D.; Choi, J.-Y.; Lee, H. Vertical Alignments of Graphene Sheets Spatially and Densely Piled for Fast Ion Diffusion in Compact Supercapacitors. *ACS Nano* **2014**, *8*, 4580−4590.
(27) Miller, J. R.; Outlaw, R. A.; Holloway, B. C. Graphene Double-Layer Capacitor with AC Line-Filtering Performance. *Science* **2010**, *329*, 1637−1639.
(28) Miller, J. R.; Outlaw, R. A.; Holloway, B. C. Graphene Electric Double Layer Capacitor with Ultra-High-Power Performance. *Electrochim. Acta* **2011**, *56*, 10443−10449.
(29) Cai, M.; Outlaw, R. A.; Butler, S. M.; Miller, J. R. A High Density of Vertically-Oriented Graphenes for Use in Electric Double Layer Capacitors. *Carbon* **2012**, *50*, 5481−5488.
(30) Bo, Z.; Yang, Y.; Chen, J.; Yu, K.; Yan, J.; Cen, K. Plasma-Enhanced Chemical Vapor Deposition Synthesis of Vertically Oriented Graphene Nanosheets. *Nanoscale* **2013**, *5*, 5180−5204.
(31) Yang, C. Y.; Bi, H.; Wan, D. Y.; Huang, F. Q.; Xie, X. M.; Jiang, M. H. Direct PECVD Growth of Vertically Erected Graphene Walls on Dielectric Substrates as Excellent Multifunctional Electrodes. *J. Mater. Chem. A* **2013**, *1*, 770−775.
(32) Cai, M.; Outlaw, R. A.; Quinlan, R. A.; Premathilake, D.; Butler, S. M.; Miller, J. R. Fast Response, Vertically Oriented Graphene Nanosheet Electric Double Layer Capacitors Synthesized from C_2H_2. *ACS Nano* **2014**, *8*, 5873−5882.
(33) Ren, W.; Cheng, H.-M. The Global Growth of Graphene. *Nat. Nanotechnol.* **2014**, *9*, 726−730.
(34) Cambaz, Z. G.; Yushin, G.; Osswald, S.; Mochalin, V.; Gogotsi, Y. Noncatalytic Synthesis of Carbon Nanotubes, Graphene and Graphite on SiC. *Carbon* **2008**, *46*, 841−849.
(35) Chen, L.; Guo, L.; Wu, Y.; Jia, Y.; Li, Z.; Chen, X. Fabrication of Vertically Aligned Graphene Sheets on SiC Substrates. *RSC Adv.* **2013**, *3*, 13926−13933.
(36) Wang, Z.; Fu, Q.; Xu, X.; Zhang, H.; Li, W.; Gao, M.; Tan, D.; Bao, X. Controlled Growth of Metal-Free Vertically Aligned CNT Arrays on SiC Surfaces. *Chem. Phys. Lett.* **2011**, *503*, 247−251.
(37) El-Kady, M. F.; Strong, V.; Dubin, S.; Kaner, R. B. Laser Scribing of High-Performance and Flexible Graphene-Based Electrochemical Capacitors. *Science* **2012**, *335*, 1326−1330.
(38) Liu, Z.; Wu, Z.-S.; Yang, S.; Dong, R.; Feng, X.; Müllen, K. Ultraflexible In-Plane Micro-Supercapacitors by Direct Printing of Solution-Processable Electrochemically Exfoliated Graphene. *Adv. Mater.* **2016**, *28*, 2217−2222.
(39) Aradilla, D.; Delaunay, M.; Sadki, S.; Gerard, J.-M.; Bidan, G. Vertically Aligned Graphene Nanosheets on Silicon Using an Ionic Liquid Electrolyte: Towards High Performance On-Chip Micro-Supercapacitors. *J. Mater. Chem. A* **2015**, *3*, 19254−19262.
(40) El-Kady, M. F.; Kaner, R. B. Scalable Fabrication of High-Power Graphene Micro-Supercapacitors for Flexible and On-Chip Energy Storage. *Nat. Commun.* **2013**, *4*, 1475.
(41) Huang, P.; Heon, M.; Pech, D.; Brunet, M.; Taberna, P.-L.; Gogotsi, Y.; Lofland, S.; Hettinger, J. D.; Simon, P. Micro-Supercapacitors from Carbide Derived Carbon (CDC) Films on Silicon Chips. *J. Power Sources* **2013**, *225*, 240−244.
(42) Hahm, M. G.; Leela Mohana Reddy, A.; Cole, D. P.; Rivera, M.; Vento, J. A.; Nam, J.; Jung, H. Y.; Kim, Y. L.; Narayanan, N. T.; Hashim, D. P.; et al. Carbon Nanotube−Nanocup Hybrid Structures for High Power Supercapacitor Applications. *Nano Lett.* **2012**, *12*, 5616−5621.
(43) Aradilla, D.; Gentile, P.; Bidan, G.; Ruiz, V.; Gómez-Romero, P.; Schubert, T. J. S.; Sahin, H.; Frackowiak, E.; Sadki, S. High Performance of Symmetric Micro-Supercapacitors Based on Silicon Nanowires Using N-methyl-N-propylpyrrolidinium Bis-(trifluoromethylsulfonyl)imide as Electrolyte. *Nano Energy* **2014**, *9*, 273−281.
(44) Thissandier, F.; Gentile, P.; Brousse, T.; Bidan, G.; Sadki, S. Are Tomorrow's Micro-Supercapacitors Hidden in a Forest of Silicon Nanotrees? *J. Power Sources* **2014**, *269*, 740−746.
(45) Li, H.; Hou, Y.; Wang, F.; Lohe, M. R.; Zhuang, X.; Niu, L.; Feng, X. Flexible All-Solid-State Supercapacitors with High Volumetric Capacitances Boosted by Solution Processable MXene and Electrochemically Exfoliated Graphene. *Adv. Energy Mater.* **2017**, *7*, 1601847.
(46) Ma, Y.; Wang, M.; Kim, N.; Suhr, J.; Chae, H. A Flexible Supercapacitor Based on Vertically Oriented 'Graphene Forest' Electrodes. *J. Mater. Chem. A* **2015**, *3*, 21875−21881.
(47) Yang, X. W.; Cheng, C.; Wang, Y. F.; Qiu, L.; Li, D. Liquid-Mediated Dense Integration of Graphene Materials for Compact Capacitive Energy Storage. *Science* **2013**, *341*, 534−537.
(48) Ben, H.; Julian, M.; Shuang, W.; Jung Bin, I.; Carlo, C.; Dimos, P.; Costas, P. G.; Roya, M. Highly Flexible, All Solid-State Micro-Supercapacitors from Vertically Aligned Carbon Nanotubes. *Nanotechnology* **2014**, *25*, 055401.

DOI: 10.1021/acsnano.7b00553
ACS Nano 2017, 11, 4009−4016